

Dinoflagellate Amphiesmal Dynamics

Subjects: [Microbiology](#)

Contributor: Alvin Chun Man Kwok , Wai Sun Chan , Joseph Tin Yum Wong

Dinoflagellates are a major aquatic protist group with amphiesma, multiple cortical membranous “cell wall” layers that contain large circum-cortical alveolar sacs (AVs). AVs undergo extensive remodeling during cell- and life-cycle transitions, including ecdysal cysts (ECs) and resting cysts that are important in some harmful algal bloom initiation–termination. AVs are large cortical vesicular compartments, within which are elaborate cellulosic thecal plates (CTPs), in thecate species, and the pellicular layer (PL). AV-CTPs provide cellular mechanical protection and are targets of vesicular transport that are replaced during EC-swarm cell transition, or with increased deposition during the cellular growth cycle.

cell wall

harmful algal blooms

cyst

dinoflagellates

amphiesma

1. Polysaccharide Deposition during Amphiesma Dynamics

Cellulose, comprising parallel unbranched β -1, 4-linked glucan chains that form microfibrils, is the major reinforcing element of plant cell walls that provides mechanical strength ^[1]. Dinoflagellate cellulose synthase *dCesA1* knockdown led to cessation of ecdysal-swarm regeneration ^[2], without flagella, suggesting cellulose synthesis dependency in the completion of amphiesma development.

C. cohnii amphiesma was stained positively for polysaccharides (CFW staining) but negatively for callose (aniline blue staining) ^[3]. The stringent chemical assay with the Updegraff protocol ^[4] demonstrated acid-resistant crystalline cellulose content being proportional to the CFW fluorescent signals (which also stained amorphous cellulose) ^[3], supporting the CTP nanomechanical hardness ^[5]. Earlier histochemical investigations using IKI/H₂SO₄ and zinc–chlor–iodide (Schultz solution), glucan assays with phenol sulfuric methods, and dissolution of isolated amphiesma preparations using basic solvents (e.g., 3%-NaOH, 100 °C for 5 h) ^{[6][7][8]} should be reinvestigated with more stringent assays, especially in relation to the co-staining of PLs.

In *Scrippsiella hexapraecingula* TEM preparations, the amphiesma was positively labeled with gold conjugated-CBHI (cellobiohydrolase I, source not mentioned, likely from *Trichoderma reesei*) and exhibited a cellulose type electron diffraction pattern ^{[9][10]}. Many cellulose-binding domain (CBDs), including bacterial CBDs (family II CEX from *Cellulomonas fimi*) and single CBHI CBD and single CBHII CBD from *Trichoderma reesei*, also bind chitin ^{[11][12][13]}, and many “cellulase” preparations contained other hydrolase activities ^{[14][15]}. The researchers further presented here CTP/PL binding with specific cellulose-binding domain (CBHI and CBDII CBDs, ^{[12][13]}) (**Figure 1A–E**). General polysaccharide dyes, including CFW, will not have this distinguishing staining. Ultrastructural studies

concerning amphiesmal polysaccharides were interpreted from “electron dense materials” that could have been targeted to either the PL or the CTPs. TEM studies on *L. polyedrum* CTP biogenesis were reviewed in [16].

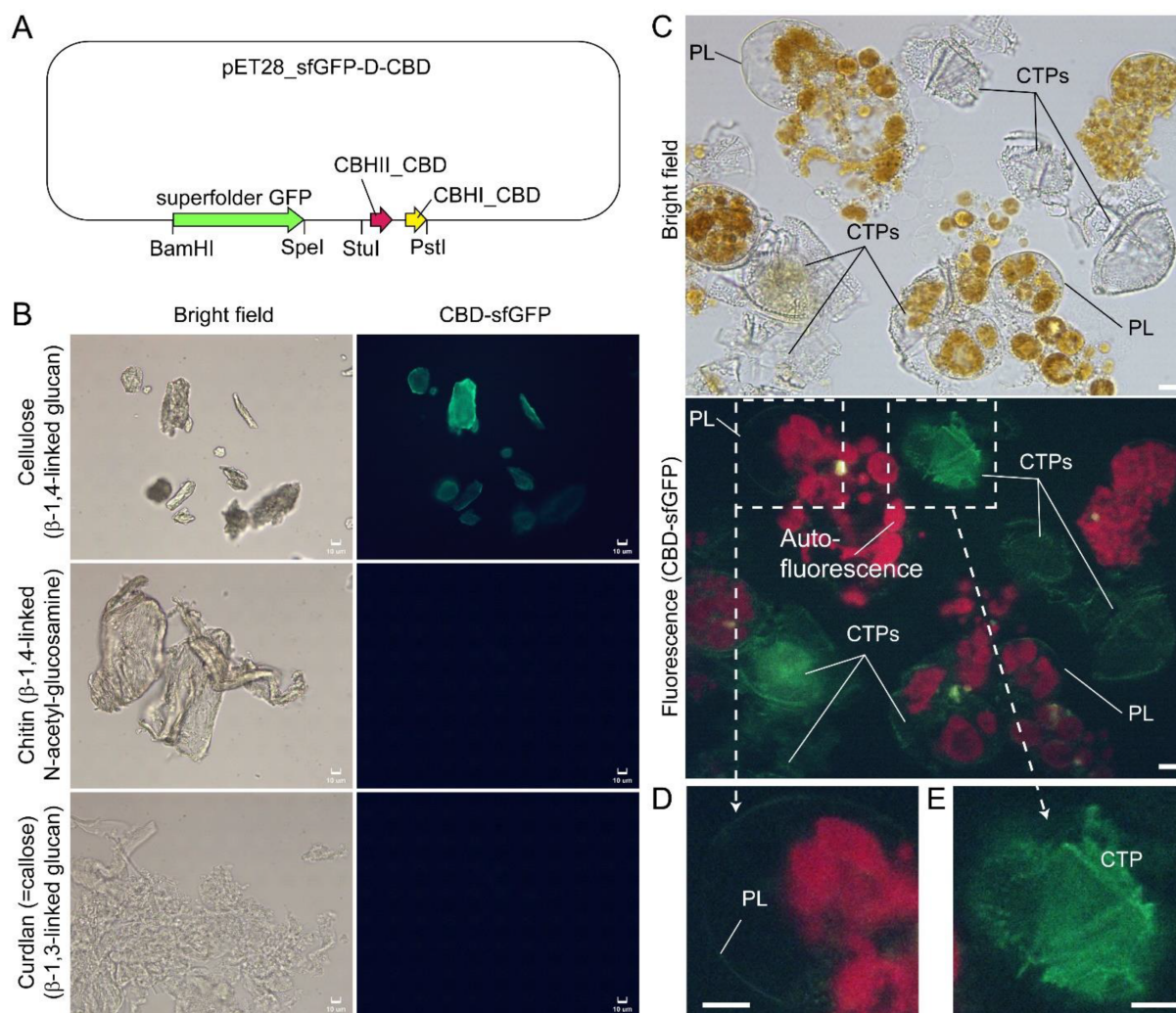


Figure 1. Compressed cell preparation of *Lingulodinium polyedrum* labeled with fluorescent recombinant cellulose-specific hybrid cellulose-binding domains. (A) Map of plasmid construct used for the generation of recombinant cellulose-specific carbohydrate-binding domain (CBD)-sfGFP fusion protein, which contained double CBDs as described in [13]. Neither single *T. reesei* CBHII CBD nor *T. reesei* CBHI CBD exhibited such specificity [12][13]. Double CBD protein was constructed by fusing the N-terminal (25–62 amino acids) of *Trichoderma reesei* CBHII CBD (AAG39980.1) to the C-terminal (478–513 amino acids) of *T. reesei* CBHI CBD (P62695.1) by a linker region of 24 amino acids (3 amino acid residues from natural CBHII linker followed by 21 amino acid residues from the natural CBHI linker). Fluorescence photomicrographs of CBD-sfGFP stained (B) microcrystalline cellulose, chitin, curdlan, and (C) *Lingulodinium polyedrum* cells (squashed gently). CTPs and pellicle (PL) were differentially stained green. Scale bar = 10 μm. (D,E) show higher-magnification views of the CBD-sfGFP-labelled (green) PL and CTP, respectively. These experiments also suggested previous single carbohydrate-binding domain non-specificity, of TEM CBD-gold labeling conducted in *Scrippsiella hexapraeicingula* [9][10], could have labeled the PL. CTPs were strongly labeled, whereas PL was not labeled except along the broken rim and after extended

exposure, which could be related to hydrophobic accumulation of the CBD domains that interact mainly by hydrophobicity.

Given the highly dynamic nature of amphiesmal membranes, the strict interpretation of cytoplasmic membrane(s), should be taken with caution as to the transiency of all developing stages, as well as to whether thinly deposited membrane(s) commence with polysaccharide deposition. Key CTP biogenesis issues are the synthesis of non-round polygonal regularity with taxonomic precision being orchestrated with normal and apolar cellular growth.

Plant cell non-cellulose polysaccharides are pre-synthesized in Golgi prior to transport and exocytotic deposition [17]. Dinoflagellate amphiesma precursors were considered to originate from some small electron-dense cortical amphisomal vesicles, which moved to the periphery of the cell, flattened, and fused together [18][19][20]. CFW readily stained CTPs/amphiesma of *Alexandrium (Gonyaulax) tamarensis* but did not label internal compartments [21]. Similarly, the lack of CFW staining in any intracellular compartments in *C. cohnii* and *L. polyedrum*, except in AV and PL [2][3], indicated there were no or undetectable matrix polysaccharides in the vesicular transport pathway.

Plant membrane-targeted cellulose synthases complexes (CSCs) catalyze glucose polymerization from the substrate UDP-glucose into cellulose polymer. The rosette CSC archetypes originated late in the chlorophyte lineage, whereas the linear archetypes remained in the non-green lineages [22][23], as was reported in dinoflagellate *Scrippsiella hexapraecingula* (although single CBD domains were deployed) [9][10]. The prominent CTPs and availability of the cyst-generation method [24][25][26], in combination with CFW-assisted flow cytometry of cellulose content in dinoflagellate cells [3], facilitated biochemical investigations of cellulose synthesis (CS) dynamics during cyst-swearer cells transition (T_{c-s}) in *L. polyedrum*. Dinoflagellate *LpCesA1* transcript was upregulated 14-fold in the early stages of ecdysal cyst regeneration, with CTPs fully regenerated between 12 and 16 h [2]. *LpCesA1* antisense knockdown in *L. polyedrum* led to abnormal thecal plate deposition and postponement of the swarmer cell regeneration [2].

2. Amphiesma Dynamics and Vesicular Transport

Polysaccharide deposition requires vesicular transport of either in-vesicle pre-synthesis or vesicular transported cellulose synthase (CesA) that mediated *on*-plasma-membrane biogenesis [27]. Ultrastructural studies suggested polyvesicular bodies (PVBs, large endosomes) commonly located close to or attached to the alveolar sacs [10][28] with fusion of these vesicles with CM constituting amphiesmal biogenesis [29].

The highly dynamic amphiesma with vesicular transport was demonstrated in the polyethylene glycol (PEG)-treatment of *on*-agar coccoidal cells [30] (**Figure 2A–D**) with which membranous layers appeared displaced when compared to control cells. Coerced cortical membrane fusion (**Figure 2B**) was observed with accelerated vesicular transport resulting in dramatic amphiesmal rearrangements [30], demonstrating the non-permanent amphiesmal nature with sustained vesicular transport dynamics.

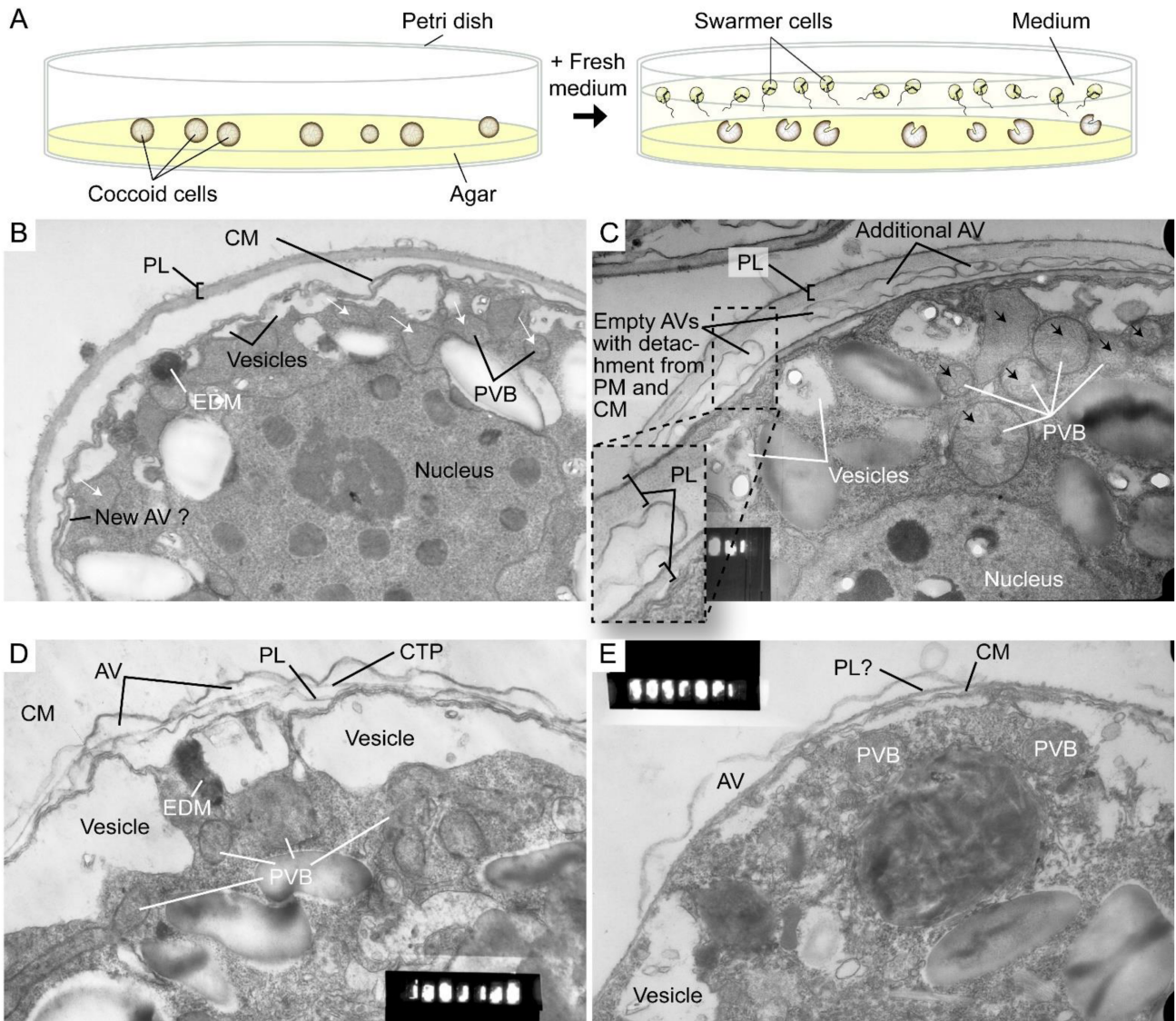


Figure 2. Amphiesmal rearrangements in coccoid cells after induced membrane fusion. **(A)** Schematic diagram showing the swarmer (daughter) and (mother) coccoid *Cryptocodinium cohnii* cells obtained by the coccoi-swarmer-release and filtration method [31]. For polyethylene glycol (PEG) treatment, cells were resuspended in 20% (*w/v*) PEG, before being spread on MLH agar plates. Transmission electron photomicrographs of the amphiesma in **(B,C)** coccoid (on agar plate) and **(D,E)** swarmer *C. cohnii* cells. Amphiesma of **(B)** control coccoid cell; **(C)** A PEG-treated coccoid cell; **(D)** A control swarmer cell and **(E)** swarmer cell released on PEG-treated plate. PEG treatment, which increased membrane fusion events [30], led to increased appearances of larger PVBs (polyvesicular bodies, large endosomes, black arrows in **(C)**) comparing to the smaller vesicles (white arrows in **(B)**) in control coccoid cells. It also drove thicker pellicular layer (PL) and amphiesmal rearrangement in the PEG-treated coccoid cell **(C)**. The PL in PEG-treated mother cell exhibited a variation from apparently one layer with polysaccharide deposition (left) to two separate membranous layers with inter vesicular bodies (unfused, right); there were also lesser stained attached vesicular bodies outside the cell. TEM sections were in the same series that were published [30] and examined with a JEOL 100CX transmission electron microscope. EDM—electron dense materials. Magnification = 19,000 \times .

The coerced increase in fusion events [30] drove the disappearance of small vesicles and the accumulation of dense material in daughter swarmer cells, demonstrating the continuum of amphiesmal dynamics with the vesicular system in mother–daughter amphiesmal transition (**Figure 2C,D**). The small vesicles in the control cells were shifted to large peri-vesicles (~4.7 times increase in volume, as measured by *ImagJ*) in PEG-treated cells (**Figure 2A,B**). The coerced fusion of the outer layers (**Figure 2D**) exhibited similarity to the zooxanthellae cell wall in hospite [32]. PEG-treated mother cells exhibited a PL thickness variation within the same cell, from apparently one layer (left) to two separate membranous layers with inter vesicular bodies (unfused, right) (**Figure 2B**), indicating PL deposition involving two membranes. There were also lesser electron dense attached vesicular bodies outside the cell, substantiating the effect of extracellular PEG in driving vesicular transport, and seconding the potential role of secretion (e.g., muco-polysaccharides) in driving vesicular transport through the decanting of cortical vesicular membranes.

Lysosensor probes, which are highly pH-sensitive, strongly labeled dinoflagellate cortices coinciding with the amphiesma (**Figure 3B**). Smaller G_1 cells appeared to have less cortical labeling when compared to the larger G_2 cells (**Figure 3C–E**) [33]. pH gradients are an important regulatory axis in the vesicular transport/secretary pathway, affecting all aspects including cargo sorting and protein processing [34][35][36][37], indicating the amphiesma's acidic pH could act as a cellular growth-deposition driver. The association of $_{CTC}[Ca^{2+}]^S$ (next section) further indicated amphiesma as a major homeostatic hub, having biochemical–biomechanical interactomes between the extracellular and intracellular environments. The researchers do not adopt acidocalcisomes to emphasize the compartments likely different from vacuolar regulation, as lysotracker and CTC staining may not fully overlap (**Figure 3A,B**). The balancing of growth, with vesicular transport, with ecdysis-attribution through secretion and oxidative potentials, will be most evident in cells with apolar–circumpolar vesicular deposition.

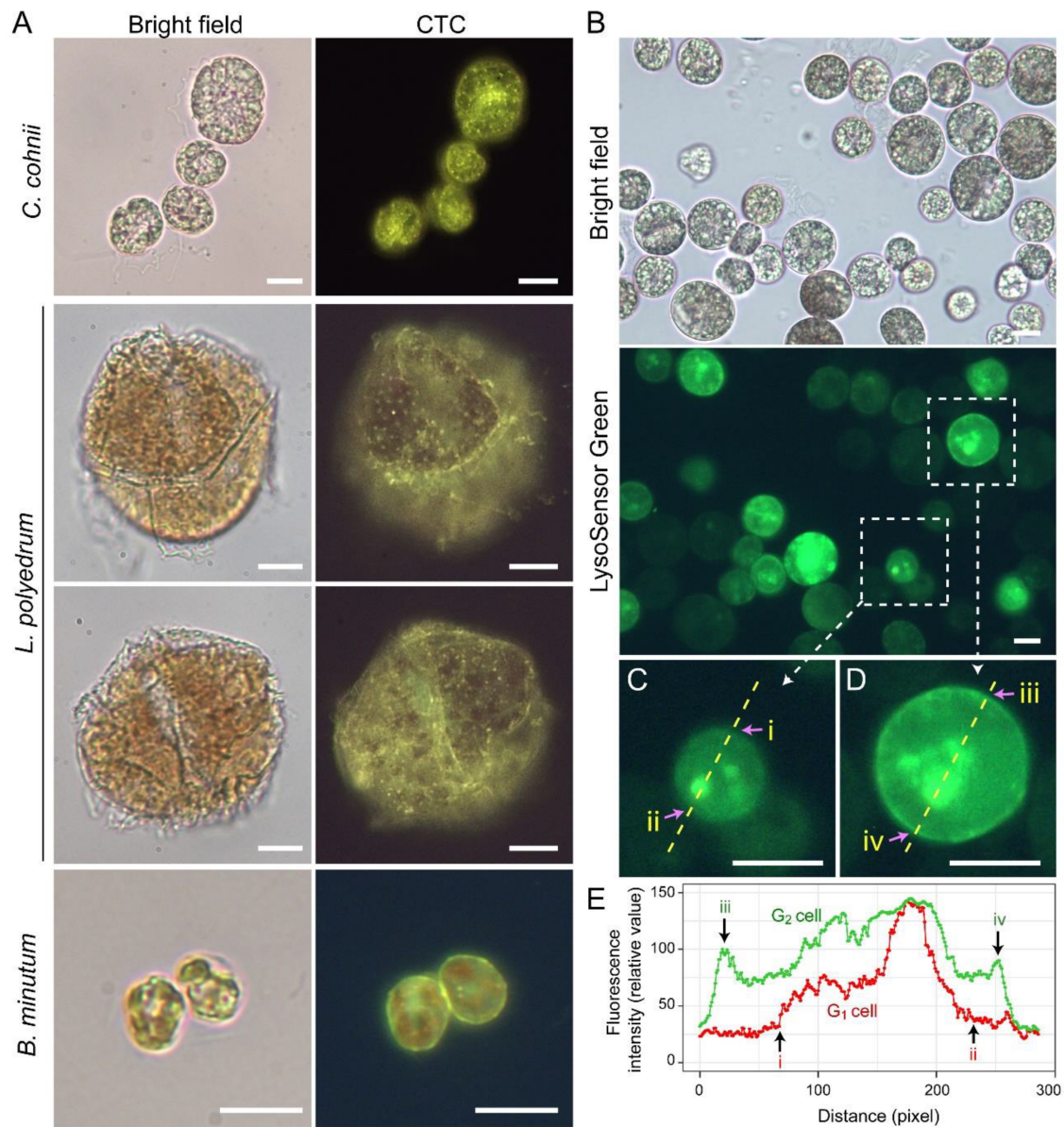


Figure 3. Amphiesma calcium stores and acidic compartments. **(A)** Fluorescence photomicrographs of chlorotetracycline (CTC)-stained *Cryptothecodinium cohnii*, *Lingulodinium polyedrum* and *Breviolum minutum* cells. Cells were briefly fixed with 1% (w/v) glutaraldehyde in seawater (5 min, 22 °C) before CTC (excitation: 380 nm, emission: 520 nm [38]) staining with brief fixation protocol [39]. Over-fixation will lead to diminishing of subcellular CTC staining, suggesting the Ca²⁺ stores were associated with active vesicular transport. CTC-positive stores were observed on the surface and distributed over the cortical layer of the cell. In addition to the tiny-dots staining pattern, CTC also stained a continuous layer in the amphiesma (yellowish-green color). CTC localization in amphiesma could be affected by inter-membrane zeta-potential and may not specially require specific Ca²⁺ binding proteins. The red fluorescence is chlorophyll autofluorescence from chloroplasts. **(B)** LysoSensor Green DND-189 (excitation: 443 nm, emission: 505 nm, 2 μM, ThermoFisher) staining yielded fewer, but larger, dots/patchy labeling in *C. cohnii*. Both cell surface and subcellular compartments were stained, with apparent increased cortical labeling in larger G₂ cells. **(C,D)** show higher-magnification views of a smaller G₁ and larger G₂ LysoSensor-stained cells, respectively. The boundaries of the G₁ cell shown in **(C)** and G₂ cell shown in **(D)** were marked by (i, ii) and (iii, iv),

respectively. (E) Quantification of fluorescent level along transects in (C,D). Smaller G_1 cells appeared to have less cortical labeling when compared to the larger G_2 cells. In either case, there were associations of inner acid compartment with the nucleus. Scale bar = 10 μm .

Microtubules are believed to play a role in thecal development [3][24], despite there are no cortical MTOCs and the cell exhibiting no apparent dynamics; they likely form a network with alveolin homologues as reported in other Alveolates [40][41][42]. Amphiesma were shed in DCB-treated dinoflagellate cells [3], an inhibitor of cellulose deposition through severing microtubular contact [43]. Actin cytoskeleton was involved in plant cellulose deposition, but cytochalasin D, an actin polymerization inhibitor, exhibited no effect in the *C. cohnii* cell growth progress (Chongping Li, unpublished data). The eleutheroschisis lack of unidirectional cytosol expansion, as required in desmoschisis, could thus directly reflect growth-vesicular transport through the whole genome-growth cycle, as there is no nuclear envelope breakdown. This was demonstrated with extracellular PEG coercing amphiesmal cortical layer emptying, rather than a selective increase in AV board thickness, suggesting the dynamic amphiesmal with exocytotic vesicular movement directly drives intracellular movement of vesicles (PVBs), the depletion of which led to empty AVs with detachment from the plasma membrane and the cytoplasmic membrane (Figure 2).

3. Calcium Signaling in Ecdysis, Cellular Growth and Bioluminescence

Cellular growth rate-dependent cADPR- Ca^{2+} signaling pathways, including dose-dependent $c_{\text{TC}}[\text{Ca}^{2+}]^{\text{S}}$ depletion, were demonstrated to orchestrate relative dinoflagellate cell growth, whereas cADPR- Ca^{2+} -store depletion mediated cortical mechanical sensitivity in dinoflagellates [39][44]. $c_{\text{TC}}[\text{Ca}^{2+}]^{\text{S}}$ mobilization exhibited pharmacological characteristics of the ciliate subplasmalemmal-like Ca^{2+} stores, a special cortical endoplasmic reticulum [45][46] that exhibits Ca^{2+} level restraint overflow from external rise [39][47]. IP_3 - Ca^{2+} signaling inhibition led to ecdysis in dinoflagellate cells [48][49][50], whereas Dantrolene (antagonist of both Ryanodine (RyR) and IP_3 receptors) efficiently blocked shaking (caffeine)-induced Ca^{2+} transient. Caffeine (cADPR receptor agonist) dose-dependently accelerated Ca^{2+} transient and plasma membrane deposition, resulting in an increase in relative cell sizes [39]. Whereas cADPR activates Ca^{2+} -SERCA to Ca^{2+} influx from cytosol, cADPR and inositol 1,4,5-trisphosphate (IP_3) commonly operate with sensitizing luminal Ca^{2+} gating of RyRs/ IP_3 R to store overload-induced Ca^{2+} release (SOICR) [51][52]. Inhibition of either one will modulate the other [53][54][55].

A dinoflagellate proton ATPase kHV1, which operated with negative Nernst potential [56][57], was proposed to function in the activation of the amphiesma associated scintillons-bioluminescence (Figure 4). Mechanically induced calcium release from intracellular Ca^{2+} store acts through the L-type Ca^{2+} channel (Figure 4), indicating the circuitry of vesicular H^+ -ATPase and L-type Ca^{2+} channels, as was shaking induced bioluminescence and mechanically induced ecdysis [28][58][59]. PLC inhibitor U73 122 blocked mechanically induced bioluminescence and indoleamine-induced IP_3 production in dinoflagellate cells [50][60], indicating also the IP_3 signaling involvement.

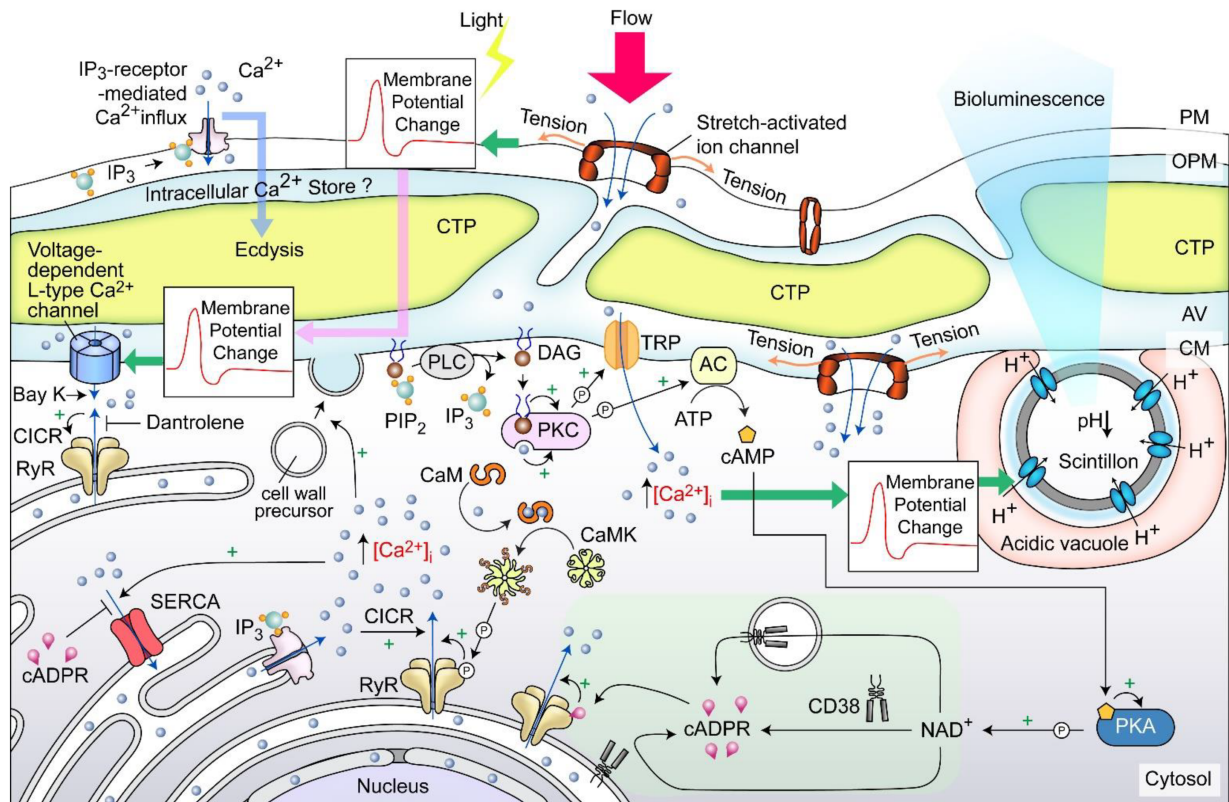


Figure 4. Amphiesma and calcium signaling. A diagrammatic representation illustrating the observations and hypothetical amphiesmal Ca^{2+} signaling pathway. The positions of the scintillon and the CTC-positive Ca^{2+} stores are arbitrary. RyR—Ryanodine receptor; PIP_2 —phosphatidylinositol 4,5-bisphosphate; IP_3 —inositol-1,4,5-trisphosphate; IP_3R — IP_3 receptor; DAG—diacylglycerol; SERCA—sarco/endoplasmic reticulum Ca^{2+} -ATPase; CICR—calcium-induced calcium release; CaM—calmodulin; CaMK— Ca^{2+} /calmodulin-dependent protein kinase; cADPR—cyclic ADP-ribose; CD38—ADP-ribosyl cyclase/cyclic ADP-ribose hydrolase; TRP—Transient receptor potential; cAMP—cyclic AMP; PKC—phospholipase C; AC—PKA—phospholipase A, P — phosphate/phosphorylation.

Mechanical shaking or the presence of fluidic mechanical forces inhibited cell proliferation of many dinoflagellates [61][62][63]. Each CTP within the surface orthogonal network of the amphiesma, with underlain cortical microtubules likely part of the mechanical sensitive system (as discussed earlier) responsible for sensing flow direction [64], and sustained stimulation could lead to depolarization, and, in turn, ecdysis or bioluminescence. This has similarity to the ciliate cortical AV-trichocyst system that is also based on AV Ca^{2+} signaling, in regulating cilia beating, including reverse swimming direction [65][66]. The intertwining between ecdysis, cellular growth, and scintillons indicates a potential bioluminescence role in dissipating oxidative stresses, as was proposed in the “oxygen defense” hypothesis [67].

References

1. Fujita, M.; Himmelspach, R.; Hocart, C.H.; Williamson, R.E.; Mansfield, S.D.; Wasteneys, G.O. Cortical microtubules optimize cell-wall crystallinity to drive unidirectional growth in *Arabidopsis*. *Plant J.* 2011, 66, 915–928.
2. Chan, W.S.; Kwok, A.C.M.; Wong, J.T.Y. Knockdown of Dinoflagellate Cellulose Synthase *CesA1* Resulted in Malformed Intracellular Cellulosic Thecal Plates and Severely Impeded Cyst-to-Swarmer Transition. *Front. Microbiol.* 2019, 10, 546.
3. Kwok, A.C.M.; Wong, J.T.Y. Cellulose synthesis is coupled to cell cycle progression at G1 in the dinoflagellate *Cryptothecodinium cohnii*. *Plant Physiol.* 2003, 131, 1681–1691.
4. Updegraff, D.M. Semimicro determination of cellulose in biological materials. *Anal. Biochem.* 1969, 32, 420–424.
5. Lau, R.K.L.; Kwok, A.C.M.; Chan, W.K.; Zhang, T.Y.; Wong, J.T.Y. Mechanical characterization of cellulosic thecal plates in dinoflagellates by nanoindentation. *J. Nanosci. Nanotechnol.* 2007, 7, 452–457.
6. Morrill, L.C.; Loeblich, A.R., III. Ultrastructure of the dinoflagellate amphiesma. *Int. Rev. Cytol.* 1983, 82, 151–180.
7. Loeblich, A.R., III. The Amphiesma or Dinoflagellate Cell Covering. In *Proceedings of the North American Paleontology Convention, Chicago, IL, USA, 5–7 September 1969*; Yochelson, E.L., Ed.; Allen Press: Lawrence, KS, USA, 1970; Volume 2, pp. 867–929.
8. Jensen, W.A. *Botanical Histochemistry, Principles and Practice*; W. H. Freeman and Co.: San Francisco, CA, USA, 1962.
9. Sekida, S.; Horiguchi, T.; Okuda, K. Development of thecal plates and, pellicle in the dinoflagellate *Scrippsiella hexapraeicingula* (Peridiniales, Dinophyceae) elucidated by changes in stainability of the associated membranes. *Eur. J. Phycol.* 2004, 39, 105–114.
10. Sekida, S.; Horiguchi, T.; Okuda, K. Development of the cell covering in the dinoflagellate *Scrippsiella hexapraeicingula* (Peridiniales, Dinophyceae). *Phycol. Res.* 2001, 49, 163–176.
11. Taylor, J.G.; Haigler, C.H.; Kilburn, D.G.; Blanton, R.L. Detection of cellulose with improved specificity using laser-based instruments. *Biotech. Histochem. Off. Publ. Biol. Stain. Comm.* 1996, 71, 215–223.
12. Linder, M.; Salovuori, I.; Ruohonen, L.; Teeri, T.T. Characterization of a Double Cellulose-binding Domain: Synergistic High Affinity Binding to Crystalline Cellulose*. *J. Biol. Chem.* 1996, 271, 21268–21272.
13. Linder, M.; Winiiecka-Krusnell, J.; Linder, E. Use of recombinant cellulose-binding domains of *Trichoderma reesei* cellulase as a selective immunocytochemical marker for cellulose in protozoa. *Appl. Environ. Microbiol.* 2002, 68, 2503–2508.

14. Ong, E.; Gilkes, N.R.; Miller, R.C., Jr.; Warren, R.A.; Kilburn, D.G. The cellulose-binding domain (CBD(Cex)) of an exoglucanase from *Cellulomonas fimi*: Production in *Escherichia coli* and characterization of the polypeptide. *Biotechnol. Bioeng.* 1993, 42, 401–409.
15. Tomme, P.; Driver, D.P.; Amandoron, E.A.; Miller, R.C., Jr.; Antony, R.; Warren, J.; Kilburn, D.G. Comparison of a fungal (family I) and bacterial (family II) cellulose-binding domain. *J. Bacteriol.* 1995, 177, 4356–4363.
16. Netzel, H.; Dürr, G. Dinoflagellate cell cortex. In *Dinoflagellates*; Spector, D.L., Ed.; Academic Press: Orlando, FL, USA, 1984; pp. 43–105.
17. Northcote, D.H.; Pickett-Heaps, J.D. A function of the Golgi apparatus in polysaccharide synthesis and transport in the root-cap cells of wheat. *Biochem. J.* 1966, 98, 159–167.
18. Morrill, L.C. Ecdysis and the location of the plasma-membrane in the dinoflagellate *Heterocapsa niei*. *Protoplasma* 1984, 119, 8–20.
19. Wetherbee, R. The fine structure of *Ceratium tripos*, a marine armored dinoflagellate. III. Thecal plate formation. *J. Ultrastruct. Res.* 1975, 50, 77–88.
20. Morrill, L.C.; Loeblich, A.R., III. Cell division and reformation of the amphiesma in the pelliculate dinoflagellate, *Heterocapsa niei*. *J. Mar. Biol. Assoc. UK* 1984, 64, 939–953.
21. Fritz, L.; Triemer, R.E. A Rapid Simple Technique Utilizing Calcofluor White M2R for the Visualization of Dinoflagellate Thecal Plates. *J. Phycol.* 1985, 21, 662–664.
22. Popper, Z.A.; Tuohy, M.G. Beyond the green: Understanding the evolutionary puzzle of plant and algal cell walls. *Plant Physiol.* 2010, 153, 373–383.
23. Tsekos, I. The sites of cellulose synthesis in algae: Diversity and evolution of cellulose-synthesizing enzyme complexes. *J. Phycol.* 1999, 35, 635–655.
24. Bricheux, G.; Mahoney, D.G.; Gibbs, S.P. Development of the pellicle and thecal plates following ecdysis in the dinoflagellate *Glenodinium foliaceum*. *Protoplasma* 1992, 168, 159–171.
25. Adamich, M.; Sweeney, B.M. The preparation and characterization of *Gonyaulax* spheroplasts. *Planta* 1976, 130, 1–6.
26. Sweeney, B.M. Freeze-fracture studies of the thecal membranes of *Gonyaulax polyedra*: Circadian changes in the particles of one membrane face. *J. Cell Biol.* 1976, 68, 451–461.
27. Paredes, A.R.; Somerville, C.R.; Ehrhardt, D.W. Visualization of cellulose synthase demonstrates functional association with microtubules. *Science* 2006, 312, 1491–1495.
28. Nicolas, M.T.; Nicolas, G.; Johnson, C.H.; Bassot, J.M.; Hastings, J.W. Characterization of the bioluminescent organelles in *Gonyaulax polyedra* (dinoflagellates) after fast-freeze fixation and antiluciferase immunogold staining. *J. Cell Biol.* 1987, 105, 723–735.

29. Melkonian, M.; Hohfeld, I. Amphiesmal Ultrastructure in *Noctiluca-Miliaris* Suriray (Dinophyceae). *Helgol. Meeresun* 1988, 42, 601–612.
30. Kwok, A.C.M.; Mak, C.K.M.; Wong, F.T.W.; Wong, J.T.Y. Novel method for preparing spheroplasts from cells with an internal cellulosic cell wall. *Eukaryot Cell* 2007, 6, 563–567.
31. Wong, J.T.Y.; Whiteley, A. An improved method for the cell cycle synchronization of the heterotrophic dinoflagellate *Cryptothecodinium cohnii*. *J. Exp. Mar. Biol. Ecol.* 1996, 197, 91–99.
32. Trench, R.K.; Blank, R.J. *Symbiodinium microadriaticum* Freudenthal, *S. goreauii* sp. nov., *S. kawagutii* sp. nov. and *S. pilosum* sp. nov.: Gymnodinioid dinoflagellate symbionts of marine invertebrates. *J. Phycol.* 1987, 23, 469–481.
33. Lam, C.M.C.; Yeung, P.K.K.; Wong, J.T.Y. Monitoring cytosolic calcium in the dinoflagellate *Cryptothecodinium cohnii* with calcium orange-AM. *Plant Cell Physiol.* 2005, 46, 1021–1027.
34. Brett, C.L.; Tukaye, D.N.; Mukherjee, S.; Rao, R. The Yeast Endosomal Na⁺(K⁺)/H⁺ Exchanger Nhx1 Regulates Cellular pH to Control Vesicle Trafficking. *Mol. Biol. Cell* 2005, 16, 1396–1405.
35. Paroutis, P.; Touret, N.; Grinstein, S. The pH of the secretory pathway: Measurement, determinants, and regulation. *Physiology* 2004, 19, 207–215.
36. Carnell, L.; Moore, H.P. Transport via the regulated secretory pathway in semi-intact PC12 cells: Role of intra-cisternal calcium and pH in the transport and sorting of secretogranin II. *J. Cell Biol.* 1994, 127, 693–705.
37. Chanat, E.; Huttner, W.B. Milieu-induced, selective aggregation of regulated secretory proteins in the trans-Golgi network. *J. Cell Biol.* 1991, 115, 1505–1519.
38. Chandler, D.E.; Williams, J.A. Intracellular divalent cation release in pancreatic acinar cells during stimulus-secretion coupling. I. Use of chlorotetracycline as fluorescent probe. *J. Cell Biol.* 1978, 76, 371–385.
39. Yeung, P.K.K.; Lam, C.M.C.; Ma, Z.Y.; Wong, Y.H.; Wong, J.T.Y. Involvement of calcium mobilization from caffeine-sensitive stores in mechanically induced cell cycle arrest in the dinoflagellate *Cryptothecodinium cohnii*. *Cell Calcium* 2006, 39, 259–274.
40. Gould, S.B.; Tham, W.H.; Cowman, A.F.; McFadden, G.I.; Waller, R.F. Alveolins, a new family of cortical proteins that define the protist infrakingdom Alveolata. *Mol. Biol. Evol.* 2008, 25, 1219–1230.
41. Gould, S.B.; Kraft, L.G.; van Dooren, G.G.; Goodman, C.D.; Ford, K.L.; Cassin, A.M.; Bacic, A.; McFadden, G.I.; Waller, R.F. Ciliate pellicular proteome identifies novel protein families with characteristic repeat motifs that are common to alveolates. *Mol. Biol. Evol.* 2011, 28, 1319–1331.
42. Tosetti, N.; Dos Santos Pacheco, N.; Bertiaux, E.; Maco, B.; Bournonville, L.; Hamel, V.; Guichard, P.; Soldati-Favre, D. Essential function of the alveolin network in the subpellicular

- microtubules and conoid assembly in *Toxoplasma gondii*. *eLife* 2020, 9, e56635.
43. Rajangam, A.S.; Kumar, M.; Aspeborg, H.; Guerriero, G.; Arvestad, L.; Pansri, P.; Brown, C.J.; Hober, S.; Blomqvist, K.; Divne, C.; et al. MAP20, a microtubule-associated protein in the secondary cell walls of hybrid aspen, is a target of the cellulose synthesis inhibitor 2,6-dichlorobenzonitrile. *Plant Physiol.* 2008, 148, 1283–1294.
 44. Lam, C.M.C.; Yeung, P.K.K.; Lee, H.C.; Wong, J.T.Y. Cyclic ADP-ribose links metabolism to multiple fission in the dinoflagellate *Cryptocodinium cohnii*. *Cell Calcium* 2009, 45, 346–357.
 45. Kissmehl, R.; Huber, S.; Kottwitz, B.; Hauser, K.; Plattner, H. Subplasmalemmal Ca-stores in *Paramecium tetraurelia*. Identification and characterisation of a sarco(endo)plasmic reticulum-like Ca²⁺-ATPase by phosphoenzyme intermediate formation and its inhibition by caffeine. *Cell Calcium* 1998, 24, 193–203.
 46. Ladenburger, E.M.; Plattner, H. Calcium-release channels in paramecium. Genomic expansion, differential positioning and partial transcriptional elimination. *PLoS ONE* 2011, 6, e27111.
 47. McCarron, J.G.; Bradley, K.N.; MacMillan, D.; Chalmers, S.; Muir, T.C. The sarcoplasmic reticulum, Ca²⁺ trapping, and wave mechanisms in smooth muscle. *News Physiol. Sci.* 2004, 19, 138–147.
 48. Tsim, S.T.; Wong, J.T.Y.; Wong, Y.H. Calcium ion dependency and the role of inositol phosphates in melatonin-induced encystment of dinoflagellates. *J. Cell Sci.* 1997, 110 Pt 12, 1387–1393.
 49. Tsim, S.T.; Wong, J.T.Y.; Wong, Y.H. Effects of dibutyryl cAMP and bacterial toxins on indoleamine-induced encystment of dinoflagellates. *Biol. Signals* 1996, 5, 22–29.
 50. Tsim, S.T.; Wong, J.T.Y.; Wong, Y.H. Regulation of calcium influx and phospholipase C activity by indoleamines in dinoflagellate *Cryptocodinium cohnii*. *J. Pineal Res.* 1998, 24, 152–161.
 51. Morgan, A.J.; Bampali, K.; Ruas, M.; Factor, C.; Back, T.G.; Chen, S.R.W.; Galione, A. Carvedilol inhibits cADPR- and IP₃-induced Ca(2+) release. *Messenger* 2016, 5, 92–99.
 52. Jiang, D.; Wang, R.; Xiao, B.; Kong, H.; Hunt, D.J.; Choi, P.; Zhang, L.; Chen, S.R. Enhanced store overload-induced Ca²⁺ release and channel sensitivity to luminal Ca²⁺ activation are common defects of RyR2 mutations linked to ventricular tachycardia and sudden death. *Circ. Res.* 2005, 97, 1173–1181.
 53. Cho, T.; Ishii-Kato, A.; Fukata, Y.; Nakayama, Y.; Iida, K.; Fukata, M.; Iida, H. Coupling of a voltage-gated Ca(2+) channel homologue with a plasma membrane H(+)-ATPase in yeast. *Genes Cells* 2017, 22, 94–104.
 54. Radhakrishnan, K.; Kamp, M.A.; Siapich, S.A.; Hescheler, J.; Luke, M.; Schneider, T. Ca(v)2.3 Ca²⁺ channel interacts with the G1-subunit of V-ATPase. *Cell Physiol. Biochem.* 2011, 27, 421–432.

55. Terland, O.; Gronberg, M.; Flatmark, T. The effect of calcium channel blockers on the H(+)-ATPase and bioenergetics of catecholamine storage vesicles. *Eur. J. Pharmacol.* 1991, 207, 37–41.
56. Kigundu, G.; Cooper, J.L.; Smith, S.M.E. Hv 1 Proton Channels in Dinoflagellates: Not Just for Bioluminescence? *J. Eukaryot Microbiol.* 2018, 65, 928–933.
57. Smith, S.M.; Morgan, D.; Musset, B.; Cherny, V.V.; Place, A.R.; Hastings, J.W.; Decoursey, T.E. Voltage-gated proton channel in a dinoflagellate. *Proc. Natl. Acad. Sci. USA* 2011, 108, 18162–18167.
58. Hardeland, R.; Burkhardt, S.; Antolín, I.; Fuhrberg, B.; Coto-Montes, A. Melatonin and 5-Methoxytryptamine in the Bioluminescent Dinoflagellate *Gonyaulax polyedra*. In *Melatonin After Four Decades: An Assessment of Its Potential*; Olcese, J., Ed.; Springer: Boston, MA, USA, 2002; pp. 387–390.
59. Hastings, J.W. Circadian Rhythms in Dinoflagellates: What Is the Purpose of Synthesis and Destruction of Proteins? *Microorganisms* 2013, 1, 26–32.
60. Lindström, J.B.; Pierce, N.T.; Latz, M.I. Role of TRP Channels in Dinoflagellate Mechanotransduction. *Biol. Bull.* 2017, 233, 151–167.
61. Thomas, W.H.; Gibson, C.H. Quantified small-scale turbulence inhibits a red tide dinoflagellate, *Gonyaulax polyedra* Stein. *Deep Sea Res. A* 1990, 37, 1583–1593.
62. Berdalet, E.; Estrada, M. Effects of turbulence on several phytoplankton species. In *Toxic Phytoplankton Blooms in the Sea, Proceedings of the 5th International Conference on Toxic Marine Phytoplankton, Newport, RI, USA, 28 October–1 November 1991*; Elsevier: Amsterdam, The Netherlands, 1993; Volume 3, pp. 737–740.
63. Berdalet, E. Effects of turbulence on the marine dinoflagellate *Gymnodinium nelsonii*. *J. Phycol.* 1992, 28, 267–272.
64. Maldonado, E.M.; Latz, M.I. Shear-stress dependence of dinoflagellate bioluminescence. *Biol. Bull.* 2007, 212, 242–249.
65. Marumo, A.; Yamagishi, M.; Yajima, J. Three-dimensional tracking of the ciliate *Tetrahymena* reveals the mechanism of ciliary stroke-driven helical swimming. *Commun. Biol.* 2021, 4, 1209.
66. Hennessey, T.M. Responses of the ciliates *Tetrahymena* and *Paramecium* to external ATP and GTP. *Purinergic Signal* 2005, 1, 101–110.
67. Wilson, T.; Hastings, J.W. *Bioluminescence: Living Lights, Lights for Living*; Harvard University Press: Cambridge, MA, USA, 2013.

Retrieved from <https://encyclopedia.pub/entry/history/show/99133>